Towards a simulation of an optically controlled microwave microstrip line at 10 GHz

Jean-Daniel Arnould, Anne Vilcot, Gérard Meunier

Toward a Simulation of an Optically Controlled Microwave Microstrip Line at 10 GHz

Jean-Daniel Arnould, Anne Vilcot, and Gérard Meunier

***Abstract*—This paper deals with a microwave microstrip line that is terminated by a laser illumination, which alters the behavior of this microwave device. The first result is the numerical simulation of the microstrip line ended by a photoinduced load with the finite element method (FEM) and with hexahedral edge elements. The main difficulties of this kind of simulation remains in the fact that we deal with an open structure and that the photoinduced load is complex and inhomogeneous.**

***Index Terms*—Anisotropic and inhomogeneous complex medium, finite element method, optical control, photoinduced load.**

I. Introduction

RECENTLY, there has been an increasing interest in applications of lightwave technology for control, generation, and measurement of microwaves [1]. Stripline configurations are especially important for the integration of electro-optic and microwave components [2]–[4]. This technique offers attractive advantages such as high isolation between the controlling optical beam and the controlled microwave signal, fast response, and high-power handling capability.

The optically controlled microwave device is made of high-resistivity silicon ($\epsilon_r = 11.7$, $\rho \approx 5000\ \Omega \cdot$ cm). We illuminate the end of the microstrip line with a laser diode whose maximum power is about 100 mW and whose wavelength is 850 nm. We observe the variation of the reflection rate $|S_{11}|$ or the transmission rate $|S_{21}|$ at high frequencies according to the intensity of the laser.

There are two ways to make numerical simulations of this structure; the first one is to simulate the illumination with an inhomogeneous zone under the microstrip line, and the second one is to program the diffusion equations in the semiconductor. The purpose of this paper is then to describe how to simulate with the FEM this kind of structure with the first method after a brief explanation of the experimentation and of the physical phenomenon.

II. Optically Controlled Microstrip Line

For the experiment, we use a microstrip line with a stub on silicon substrate whose geometrical characteristics are shown in Fig. 1. We apply an optical signal at the end of the stub. We study the effect of the optical power on the transmission rate $|S_{21}|$ between 500 MHz and 10 GHz, as shown in Fig. 2, where $|S_{21}|^2 = |P_{\rm out}/P_{\rm in}|$.

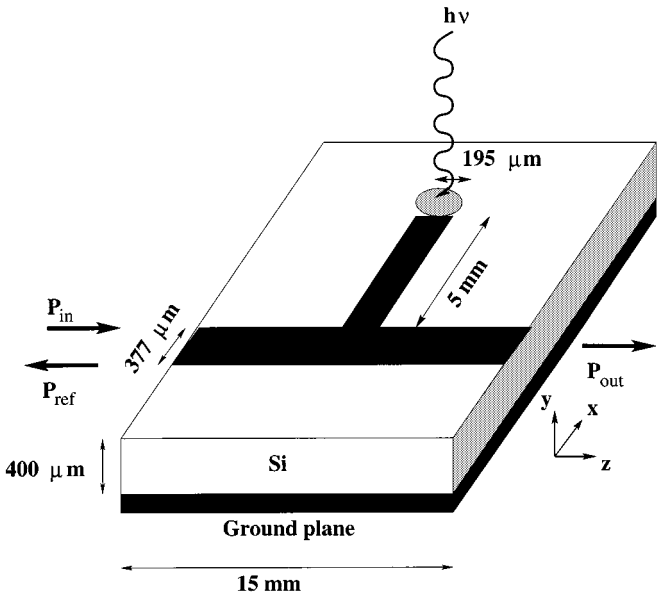

Fig. 1. Physical characteristics of the microstrip line 50 Ω.

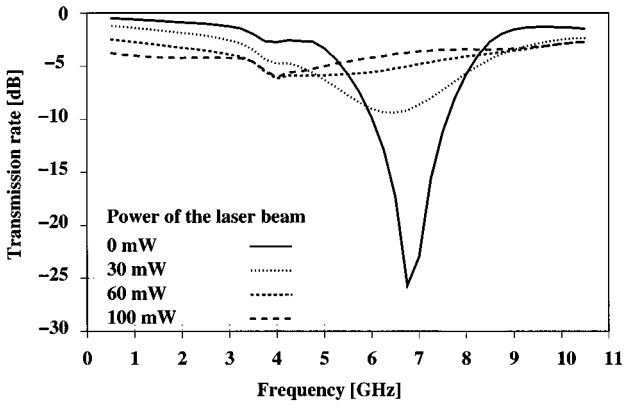

Fig. 2. Transmission rate $|S_{21}|$ of the microstrip line.

We can say that the stub is like a resonant line terminated by a load whose complex impedance varies with the optical power; the silicon conductivity is locally modified by the laser beam [5]. When the laser illuminates the silicon at the end of the line, the light is absorbed, and electron–hole pairs are generated. On the influence of the electric field and because of the concentration gradient, the carriers move into the silicon. This diffusion can be lateral as well as vertical, but in the depth of the silicon, the process of recombination proceeds.

Manuscript received July 5, 2001; revised October 25, 2001.

J.-D. Arnould and A. Vilcot are with the Laboratoire d'Electromagnétisme, Microondes et Optoélectronique, UMR CNRS 5530, ENSERG/INPG, Grenoble, France (e-mail: arnould@enserg.fr).

G. Meunier is with the Laboratoire d'Electrotechnique de Grenoble, UMR CNRS 5529, ENSIEG/INPG, Saint-Martin d'Hères, France.

Publisher Item Identifier S 0018-9464(02)00907-X.

III. Explanation of the Physical Phenomenon

This section consists of a brief explanation of the physical phenomenon and a presentation of the interaction between microwave and optical signals.

Three basic equations govern the semiconductor device, the Poisson's equation (1), the transport equations (2), and the conduction and diffusion current equations (3).

In our case, the Poisson equation can be expressed by

$$\nabla \cdot \mathbf{E} = -\frac{e(\Delta n - \Delta p)}{\epsilon_p} \tag{1}$$

where $\mathbf{E}$ is the electric field, $\epsilon_p = \epsilon_0 \epsilon_{pr}(x, y, z, t)$ is the permittivity of the plasma, and $\Delta n = n - n_0$ and $\Delta p = p - p_0$ are the excess density of carriers.

The transport equations can be expressed by

$$\begin{cases} \dfrac{\partial n}{\partial t} = \dfrac{1}{e}, & \nabla \mathbf{J_n} + g_n - r_n \\ \dfrac{\partial p}{\partial t} = -\dfrac{1}{e}, & \nabla \mathbf{J_p} + g_p - r_p \end{cases} \tag{2}$$

where $i = n, p$ design the density of carriers (respectively, electrons or holes), J_i is the current density of carriers, g_i is the generation rate of carriers, and r_i is the recombination rate of carriers.

Finally, the sum of the conduction current $\mathbf{J_{ci}}$ and the diffusion current $\mathbf{J_{di}}$ equations is for each carrier $i = n, p$:

$$\begin{cases} \mathbf{J_n} = \mathbf{J_{cn}} + \mathbf{J_{dn}} = ne\mu_n \mathbf{E} + eD_n \nabla n \\ \mathbf{J_p} = \mathbf{J_{cp}} + \mathbf{J_{dp}} = pe\mu_p \mathbf{E} - eD_p \nabla p \end{cases} \tag{3}$$

where D_i is the diffusion constant of carriers, and μ_i is the mobility of carriers.

When a semiconductor is submitted at a high frequency wave, we cannot neglect the drift current density $\mathbf{J_{drift}} = \jmath\omega\epsilon\mathbf{E}$ compared with the conduction current density $\mathbf{J_c} = \mathbf{J_{cn}} + \mathbf{J_{cp}} = \sigma\mathbf{E}$ and the diffusion current density $\mathbf{J_d} = \mathbf{J_{dn}} + \mathbf{J_{dp}}$. The total current density proportional to $\mathbf{E}$ is then $\mathbf{J_t} = \mathbf{J_c} + \mathbf{J_{drift}} = \jmath\epsilon_0\epsilon_{pr}\mathbf{E}$ and with the plasma theory [2], we have

$$\epsilon_{pr} = \epsilon_r - \frac{\omega_p^2 \tau^2}{1 + \omega^2 \tau^2} - \jmath \frac{\omega_p^2}{\omega} \frac{\tau}{1 + \omega^2 \tau^2} \tag{4}$$

where $\epsilon_r = 11.7$ is the initial permittivity, τ is the mean time between two collisions, ω_p is the plasma frequency, and ω is the microwave frequency.

We have to make some assumptions to solve those complex equations because we have three unknown vectors ($\mathbf{E}(x, y, z, t)$, $\mathbf{J_n}(x, y, z, t)$, $\mathbf{J_p}(x, y, z, t)$) and two unknown scalars ($n(x, y, z, t)$, $p(x, y, z, t)$).

A. Assumptions

The problem consists of calculating the photo-induced load placed at the end of the transmission line through the relative plasma permittivity ϵ_{pr}, which is a function of the carrier concentrations. We assume that the carriers are photogenerated in pairs and that the ambipolar diffusion model (which is equivalent to the electric neutrality) and the Shockley–Read–Hall statistic are checked [6]. We can solve with (2) and (3) the ambipolar diffusion equation in the y way:

$$D_a \frac{\partial^2 \Delta n}{\partial y^2} + \mu_a \frac{\partial(\mathbf{E}\Delta n)}{\partial y} + g_a - r_a = \frac{\partial \Delta n}{\partial t} \tag{5}$$

with

$$D_a = \frac{(p+n)D_n D_p}{pD_p + nD_n}, \quad \mu_a = \frac{(p-n)\mu_n \mu_p}{p\mu_p + n\mu_n}, \quad r_a = \frac{\Delta n}{\tau}$$

and

$$g_a = g_0 \exp^{-(y/y_0)}$$

where y_0 is the penetration depth, g_0 is the generation rate at the surface, and τ is the lifetime.

Neglecting the term in $\mathbf{E}$ and under constant illumination, we can resolve this equation in steady state as

$$\Delta n = A \exp^{-(y/L_a)} + B \exp^{(y/L_a)} + C \exp^{-(y/y_0)} \tag{6}$$

where A, B, and C are constants to be determined by the boundary conditions (surface recombination speed [7]), and $L_a = \sqrt{D_a \tau}$ is the ambipolar diffusion length.

B. Parameters Used in the Simulation

Because of the uncertainty on the value of certain parameters, we set them to their usual values and we observe the effect of their modification of the other parameters. We can show the initial values of the parameters on Table I.

TABLE I
Initial Values

Carriers	Electron	Holes
Doping concentration n_0, p_0 $[cm^{-3}]$	$3.8\,10^7$	$2.6\,10^{12}$
Mobility μ_n, μ_p $[cm^2.(VS)^{-1}]$	1350	480
Diffusion constant D_n, D_p $[cm^2.s^{-1}]$	34.9	12.4
Mean time τ_{n0}, τ_{p0} $[ps]$	0.221	0.13

We can distinguish two zones in the semiconductor.

At the surface of the semiconductor, we have the strong injection mode ($\Delta n = \Delta p \gg p_0, n_0$).

Then, $\tau \approx 2\tau_{n0} \approx 2\tau_{p0}$, $\mu_a = 0$, and $D_a = 2D_n D_p/(D_n + D_p)$.

In the depth of the semiconductor near the ground plane, we have the low injection mode ($\Delta n \ll p_0$), and the conductive current is due to electron move (which is the lower carrier).

Then, $\tau = \tau_{n0}$, $\mu_a = \mu_n$, and $D_a = D_n$.

We study the strong injection mode. The term A is dominant in (6) for $y \in [0; 350\ \mu\text{m}]$:

$$n(y) - n_0 = p(y) - p_0 = n_s \exp^{-(y/L_a)} \tag{7}$$

where $n_s = p_s = 4\ 10^{15}\ \text{cm}^{-3}$ is the carrier concentration at the surface of the semiconductor (depending on $P_{\text{lum}} = 12.8$ mW·cm^{-2} and $\lambda_{\text{lum}} = 850$ nm) [6].

Equation (4) can be simplified in the way of the electric polarization and for $f = \omega/2\pi < 12$ GHz:

$$\epsilon_{pr}(y) = \epsilon_r - \jmath \left(\frac{p(y)e^2}{\epsilon_0 m_p^*} \frac{\tau_p}{\omega} + \frac{n(y)e^2}{\epsilon_0 m_n^*} \frac{\tau_n}{\omega} \right). \tag{8}$$

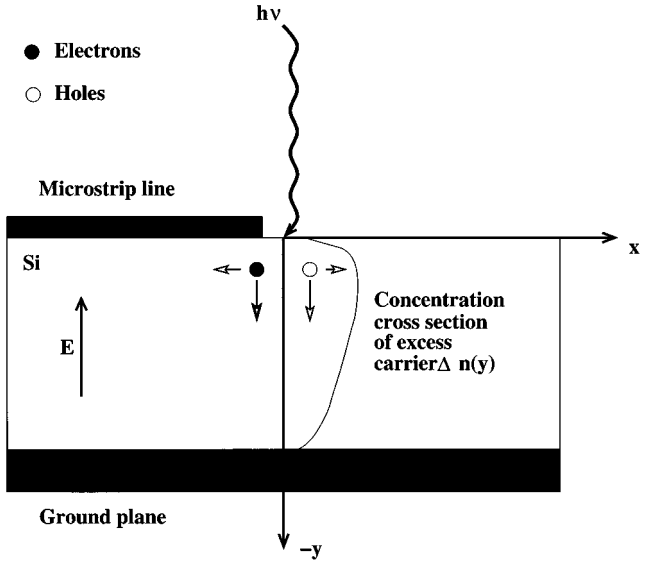

Fig. 3. Concentration cross section of the excess carrier.

For a mean time $\tau = 2\tau_{n0}$, we can evaluate the ambipolar diffusion length $L_a = 285\ \mu$m. We can see, with these parameters, the resulting cross section of excess carrier on Fig. 3.

IV. Numerical Simulation

We begin the simulation of this structure with a microstrip line without illumination. The physical dimensions are the same as shown in Fig. 1. For this, we use the FEM with hexahedral edge elements and electric walls far enough from the microstrip in order not to disturb the electromagnetic field. The weak problem can be written with the classic electric formulation [8] as

$$\begin{cases} \text{Find } \mathbf{E} \in H(\text{curl}) = \left\{\mathbf{A} \in \mathbb{L}^{\mathbf{2}}(\mathbf{\Omega});\ \nabla \times \mathbf{A} \in \mathbb{L}^{\mathbf{2}}(\mathbf{\Omega})\right\} \\ \displaystyle\int_{\Omega} \mu_r^{-1}(\nabla \times \mathbf{E}).(\nabla \times \mathbf{W})\, d\Omega - k_0^2 \int_{\Omega} \epsilon_{pr}\mathbf{E}.\mathbf{W}\, d\Omega \\ \quad = -jw\mu_0 \displaystyle\int_{S_e} \mathbf{Je}.\mathbf{W}\, dS \\ \forall \mathbf{W} \in H(\text{curl}) \end{cases} \tag{9}$$

where $\mathbf{W}$ is a test function, $\mathbf{E}$ is the electric field, k_0 is the wave number, $\mathbf{Je}$ is the electric current density source, $\epsilon_{pr} = \epsilon_{pr}(r, y)$ is the relative plasma permittivity given by (8), and $\mathbb{L}^2(\Omega) = \{(\mathbf{A})\colon \mathbf{\Omega} \to \mathbf{C^3}; \int_{\Omega} |\mathbf{A}|^{\mathbf{2}}\, \mathbf{d\Omega} < \infty\}$.

The edge elements are well suitable to simulate high-frequency problems because the continuity of the electric field between the dielectrics is intrinsic, and the parasite modes of higher order are eliminated [8]. First-order complete hexahedral elements are used to conform to the global geometry of the simulated structure.

In three dimensions, we must consider the radius position r of carriers

$$\Delta n(r, y) = \Delta n(y) \exp^{(-r/R_0)} \tag{10}$$

where $\Delta n(y)$ is given by (7), $R_0 = 20\ \mu$m, which is the radius of the spot laser at the surface of the silicon.

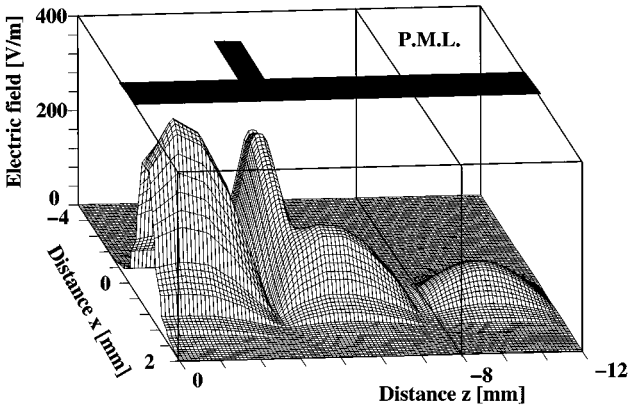

Fig. 4. Electric field propagation at the plane $y = 200\ \mu$m.

The electric current density source $\mathbf{Je}$ is calculated in two dimensions to impose the correct mode in the structure with the classic formulation $\nabla \cdot (\epsilon \nabla V) = 0$ [9].

To calculate the S parameter, which is the ratio between the reflected or the transmitted power, we have two different methods,when the access are matched.

The difficulty is to separate the incident wave from the reflected wave or the transmitted wave since we obtain the sum of them.

The first solution is to use the method of the perfectly matched layer (PML), which can be considered to be a matched load [10]. In this way, there is no reflected wave. Equation (11) shows that the PML is like a special material with complex anisotropic permittivity $\epsilon^{(2)}$ and permeability $\mu^{(2)}$.

$$\epsilon^{(2)} = \epsilon_0 \begin{bmatrix} \epsilon_r^{(1)} a_{\text{pml}} & 0 & 0 \\ 0 & \epsilon_r^{(1)} a_{\text{pml}} & 0 \\ 0 & 0 & \epsilon_r^{(1)}/a_{\text{pml}} \end{bmatrix}$$
$$\mu^{(2)} = \mu_0 \begin{bmatrix} a_{\text{pml}} & 0 & 0 \\ 0 & a_{\text{pml}} & 0 \\ 0 & 0 & 1/a_{\text{pml}} \end{bmatrix} \tag{11}$$

where $a_{\text{pml}} = \epsilon^{(2)}/\epsilon^{(1)}$ is an arbitrary complex constant that fixes the strength of the attenuation in the PML medium $^{(2)}$ compared with the medium $^{(1)}$, which is here either air or silicon [11].

We can notice that PML has been used at the end of the stub to simulate a infinite line; the wave is absorbed at the end of the structure with a matched load, as shown in Fig. 4.

Two PML areas are necessary: the first one to attenuate the wave propagation at the end of the air area and the second one to attenuate the wave propagation in the silicon area.

The second method uses a linear combination of elementary solutions from (9). This method requires a number of resolutions equal with the number of accesses [12].

V. Numerical Results

Without illumination at the end of the stub, the value of the silicon relative permittivity is simple and homogeneous in three dimensions: $\epsilon_r = 11.7 - j(4.504\,10^8/f)$ according to (8).

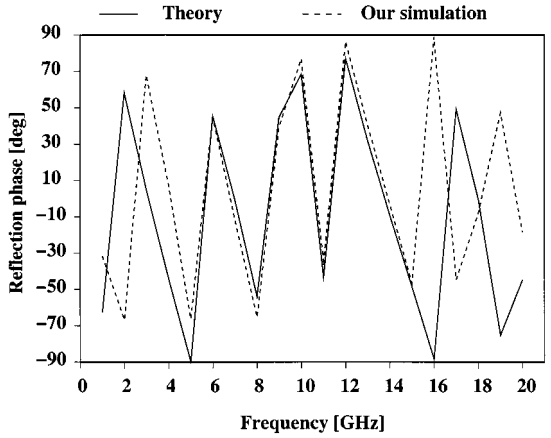

Fig. 5. Reflection phase S_{11} of the microstrip line with the stub.

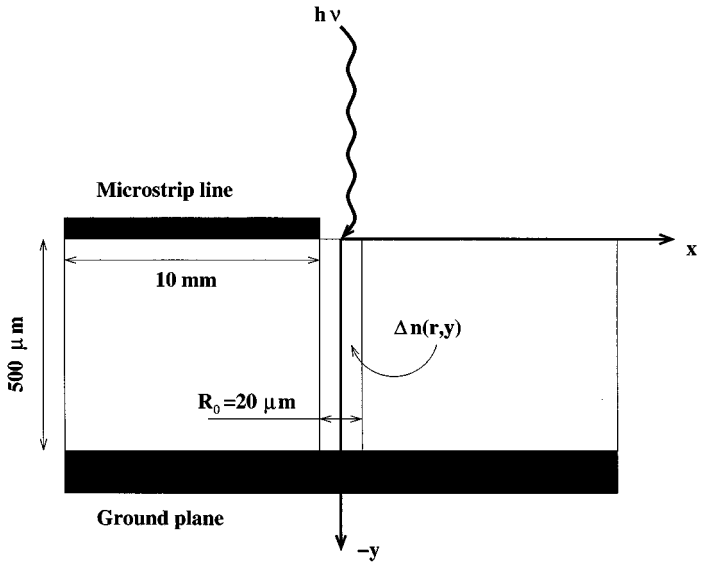

Fig. 6. Physical parameters with illumination.

To test the validity of the formulation (9), we begin to simulate the microstrip line with the stub, as shown in Fig. 5 without illumination.

First-order complete hexahedral elements are used to conform to the global geometry of the simulated structure.

We have checked that electric walls used to limit the domain of simulation according to $y = 2$ mm, $x = 2$ mm, and $x = -4$ mm have no influence on the calculation of the electromagnetic field near the microstrip line.

After 15 GHz, the meshing of the open structure could not be fine enough and explains the difference between our simulation and theory.

To test if the developed tool is able to take the photoconductivity losses into consideration, we simulate at 10 GHz an open microstrip line terminated with an inhomogeneous complex medium given by (10), as shown in Fig. 6.

Without illumination, the reflection rate is $S_{11} = 0$ dB, and with an illumination corresponding to the parameters given by (8) and by (10), the reflection rate is $S_{11} = -2$ dB, which is a good value according to the experiment.

VI. Conclusion

We have presented in this paper the complex open problem of the simulation of a microwave microstrip line that is enlightened with a laser beam. The tools are developed to simulate the open structure at high frequencies (about 10 GHz) with electric and magnetic walls and inhomogeneous complex load. The simulations with hexahedral edge elements are encouraging, with the microstrip line and the PML. We have to do many more simulations with different frequencies and optical power to compare with measurements that will refine the model of the complex photoinduced load.

References

[1] V. A. Manasson, L. S. Sadovnik, and V. A. Yepishin, "An optically controlled mmw beam-steering antenna based on a novel architecture," *IEEE Trans. Microwave Theory Tech.*, vol. 45, pp. 1497–1500, Aug. 1997.

[2] C. H. Lee, P. S. Mak, and A. P. Defonzo, "Optical control of millimeter-wave propagation in dielectric waveguides," *IEEE J. Quantum Electron.*, vol. QE-16, pp. 277–288, Mar. 1980.

[3] H. Shimasaki and M. Tsutsumi, "Reflection characteristics of optically-controlled microwave through an open-ended microstrip line," *IEICE Trans. Electron.*, vol. E76-C, no. 2, pp. 301–304, Feb. 1993.

[4] M. Serres, I. Huynen, and A. Vander Vorst, "Wide-band modeling of photoinduced carriers at the end of an open-ended microstrip line," *IEEE J. Select. Topics Quantum Electron.*, vol. 4, pp. 948–952, Nov./Dec. 1998.

[5] B. Boyer, J. Haidar, A. Vilcot, and M. Bouthinon, "Tunable microwave load based on biased photoinduced plasma in silicon," *IEEE Trans. Microwave Theory Tech.*, vol. 45, pp. 1362–1367, Aug. 1997.

[6] S. S. Li, *Semiconductor Physical Electronics*. New York: Plenum, 1993.

[7] M. Shur, *Physics of Semiconductor Devices*. Englewood Cliffs, NJ: Prentice-Hall, 1990.

[8] N. J. L. Yao Bi, "Méthode des éléments finis mixtes et conditions absorbantes pour la modélisation des phénomènes électromagnétiques hyperfréquences," Ph.D. dissertation, Ecole Centrale Lyon, Lyon, France, 1995.

[9] M. Aubourg, "Méthode des éléments finis appliquée à des problèmes de propagation d'ondes électromagnétiques guidées," Ph.D. dissertation, Univ. Limoges, Limoges, France, July 1985.

[10] J. P. Berenger, "A perfectly matched layer for the absorption of electromagnetic waves," *J. Comput. Phys.*, pp. 185–200, 1994.

[11] A. Mitchell, J. T. Aberle, D. M. Kokotoff, and M. W. Austin, "An anisotropic pml for use with biaxial media," *IEEE Trans. Microwave Theory Tech.*, vol. 47, pp. 374–377, Mar. 1999.

[12] E. Marouby, "Analyse d'élements de connectique microondes par la méthode des éléments finis," Ph.D. dissertation, Univ. Limoges, Limoges, France, Apr. 1990.